Journal of Sound and Vibration (2000) **238**(3), 481–494
doi:10.1006/jsvi.2000.3210, available online at http://www.idealibrary.com on IDEAL®

A NEW PERSPECTIVE FOR SEMI-AUTOMATED STRUCTURAL VIBRATION CONTROL

N. JALILI

Department of Mechanical Engineering, Clemson University, Clemson, SC 29634-0921, *U.S.A.*

(*Received* 15 *October* 1999, *and in final form* 22 *June* 2000)

The development of an innovative approach for optimum vibration suppression of flexible structures is presented. Utilizing concurrent use of semi-active and active subsections, an intelligent *semi-automated* alternative is suggested. By altering the adjustable structural properties (in semi-active unit) and control parameters (in active unit), a search is conducted to minimize an objective function subject to constraints, which may reflect performance characteristics. In practice, a *user-in-the-loop* interprets the resulting performance. A number of options may then be initiated: altering the parameters of the semi-active unit, or re-tuning the control parameters in the active unit, or concurrently adjusting the two. An essential component of this strategy is handling the parametric variations within the system. In order to increase the absorber efficiency against such variations an identification process is utilized in sequence with an optimization for re-tuning the absorber. The feasibility of the re-tuning procedure and performance improvement is demonstrated via simulations for a single-degree-of-freedom (s.d.o.f.) system. It is shown that concurrent adjustment of structural properties and control re-tuning significantly improves the vibration suppression quality.

1. MOTIVATION AND PROBLEM STATEMENT

During recent years, vibration suppression schemes such as those with passive, semi-active, and active devices have attracted interest in engineering research and development. In passive methods, an attempt is made to optimize the structure's properties (such as damping), while active methods try to alternate the vibration (by damping or cancellation) without considering the power requirement constraint [1–5]. Much attention is being paid to the semi-active approaches for their low-energy requirement and cost. Recent advances in smart materials and adjustable dampers and absorbers have significantly contributed to the applicability of these approaches [6–8].

Although much progress has been made, hybrid systems, i.e., combination of semi-active and active treatments deserves more investigation and research. Many semi-active or active vibration absorption techniques have been developed, but the study of an intelligent combination of the two has been overlooked [9, 10]. From the design perspective, the drawback of most vibration suppression schemes is that they only provide performance characteristics of systems whose parameters have been specified. Design optimization, parametric studies, and sensitivity analyses that need re-formulating procedure are difficult, if not impossible to perform. These methods become difficult and time-consuming for complex systems and could introduce non-intuitive behavior in active elements [11, 12].

In this study, an innovative design approach is suggested for this hybrid treatment (semi-active/active), in which the advantages of individual schemes are combined while eliminating their shortfalls. The semi-active subsection could include smart structures

0022-460X/00/480481 + 14 $35.00/0

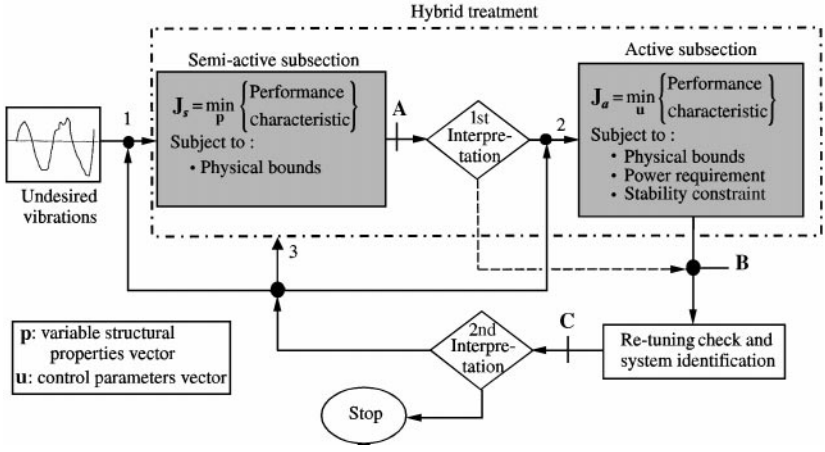

Figure 1. Schematic of the semi-automated treatment.

ranging from ER/MR dampers to magnetostrictive actuators, and a particular set of piezoelectric actuators may form the active subsection. By altering the adjustable structural properties (in semi-active unit) and control parameters (in active unit), a search is conducted to minimize an objective function subject to certain constraints, which may reflect the performance characteristics.

Figure 1 illustrates the schematic of this semi-automated vibration suppression process, where an interpretation stage is introduced in practice. Utilizing this interpretation, an attempt is made to suppress the amplitude of vibrations in the semi-active unit to the extent possible. This is the least power-consuming effort, and an attempt is made to adjust the structural properties (which are variable) such that a vibration absorption measure (mean square acceleration response, for instance) is minimized. Due to the physical constraints and design considerations, this optimization is forced to result in feasible properties.

As soon as this semi-active adjustment is completed (**A** in Figure 1), the first interpretation is performed on the suitability of the vibration suppression performance. If necessary, the control parameters (in the active unit) will be adjusted so that the remaining vibration suppression requirement is achieved. This optimization is also subjected to physical bounds, a desired energy requirement, and stability constraints. The energy constraint will introduce a trade-off between vibrations suppression quality and power consumption.

It should be noted that if the vibration suppression were satisfied in the semi-active subsection, the active unit could be bypassed (dashed lines from the 1st interpretation to **B** in Figure 1). If further improvement is needed (not achievable through a semi-active unit) or the resultant structural properties are not desirable, this active unit will trigger to alter the control parameters, as shown in Figure 1.

A re-tuning check followed by the system identification is performed, next, (**B** in Figure 1), for detecting possible variations in the system parameters. This re-tuning check is needed when the absorber structures deviate from their nominal design, or structural features of the primary alter, or both. The 2nd interpretation, **C** in Figure 1, is now performed to re-tune the control parameters and/or structural properties based on the resulting system identification. There are three possible options to follow: to use (1) only semi-active adjustment; (2) only control re-tuning; or (3) concurrent semi-active adjustment of

structural properties and control parameters re-tuning (see corresponding ports in Figure 1).

An interesting feature of the active unit is the re-tuning of the control parameters. By simple re-tuning of the control parameters, frequent changes of the variable dampers and absorbers in the semi-active unit can be avoided (from the 2nd interpretation to port 2 in Figure 1). This re-tuning is repeated until no significant changes in the parameters are observed. The main contribution of this study is introducing this interpretation and demonstrating its feasibility through simulations. The predominant activity will be around developing and facilitating this interpretive decision-making process via numerical tools, and when implemented on realistic systems with complex dynamics and controllability.

The paper is organized as follows: in the immediately following section, an analytical model is developed for a single-degree-of-freedom (s.d.o.f.) primary in presence of parametric uncertainties, and subjected to a wide-band excitation force. Section 3 addresses the optimization process over the structural properties and control parameters with the associated stability and physical constraints. The issues regarding parametric identification and the re-tuning problem are discussed in section 4. Section 5 presents the numerical examples, and section 6 concludes the study and points out the future directions.

2. MATHEMATICAL MODELLING

In order to explain the underlying concept, an example structure is considered: a s.d.o.f. primary system equipped with an s.d.o.f. absorber attachment, for suppressing undesired oscillations caused by wide-band force excitations (see Figure 2). The absorber consists of adjustable parameters (spring, k_a, and damper, c_a) and the active component, $u(t)$.

The governing dynamics is expressed as

$$m_a\ddot{x}_a(t) + c_a\dot{x}_a(t) + k_a x_a(t) - u(t) = c_a\dot{x}_1(t) + k_a x_1(t), \tag{1}$$

$$m_1\ddot{x}_1(t) + (c_1 + c_a)\dot{x}_1(t) + (k_1 + k_a)x_1(t) - \{c_a\dot{x}_a(t) + k_a x_a(t) - u(t)\} = f(t), \tag{2}$$

where $x_1(t)$ and $x_a(t)$ are the respective primary and absorber displacements, and $f(t)$ is the excitation force. The control $u(t)$ represents a generic feedback control with vector of parameters $\mathbf{u}$. We also define a vector $\boldsymbol{\theta} = \{m_a\ c_a\ k_a\ m_1\ c_1\ k_1\}^{\mathrm{T}}$ of the system parameters whose components are indicated in Figure 2. Notice that only vector $\mathbf{p} = \{c_a\ k_a\}^{\mathrm{T}}$ is considered to have adjustable features in the semi-active unit.

It is assumed that the *true value* of $\boldsymbol{\theta}$, say $\boldsymbol{\theta}^*$, is unknown, but bounded. That is,

$$\|\Delta\boldsymbol{\theta}/\bar{\boldsymbol{\theta}}\| \leqslant \psi, \tag{3}$$

where $\|\ \|$ denotes a vector norm, / represents a term-by-term division, ψ is a positive finite scalar,

$$\Delta\boldsymbol{\theta} = \boldsymbol{\theta}^* - \bar{\boldsymbol{\theta}} = \begin{cases} \Delta m_a = m_a^* - \bar{m}_a, \\ \Delta c_a = c_a^* - \bar{c}_a, \\ \Delta k_a = k_a^* - \bar{k}_a, \\ \Delta m_1 = m_1^* - \bar{m}_1, \\ \Delta c_1 = c_1^* - \bar{c}_1, \\ \Delta k_1 = k_1^* - \bar{k}_1, \end{cases} \tag{4}$$

and $(\ )^*$ and $(\bar{\ })$ denote the respective *true* and *nominal* values of the argument.

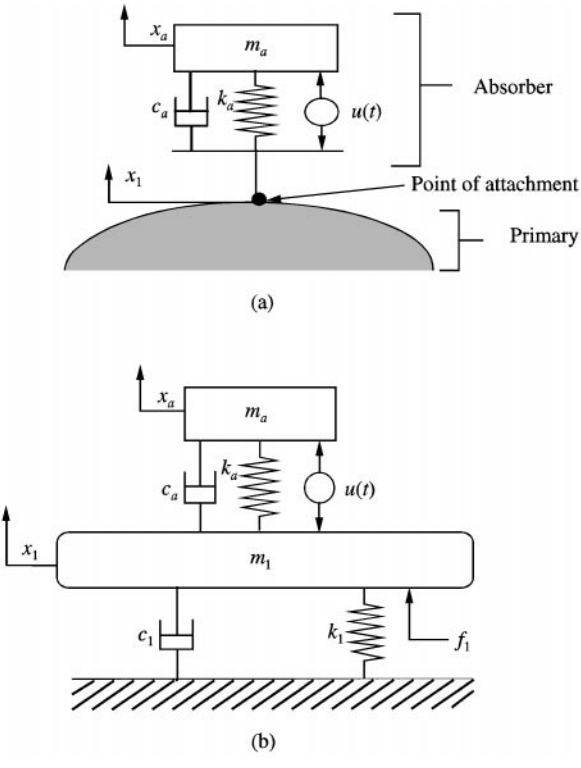

Figure 2. (a) A general and (b) s.d.o.f. model of the primary structure equipped with absorber.

Utilizing the Laplace domain representation of the system of equations (1) and (2), for a selected control law $u(t)$, the required transfer function between primary acceleration and excitation force (output–input relation),

$$H(s) = s^2 X_1(s)/F(s), \tag{5}$$

can be the obtained (see equation (A.1) in Appendix A).

Notice the characteristic equation of the combined system is simply the denominator of the transfer function $H(s)$. The passive absorber, i.e., $u = 0$, is always stable. The stability issue arises when active control is used. As the control parameters **u** are used for optimization, their influence on the system stability should be studied in parallel.

The main objective of this study is to design an optimum vibration absorber for wide-band frequency excitation. The optimum absorber performance is achieved by minimizing a selected performance characteristic over the absorber structural properties, **p**, and control parameters, **u**, as described next.

3. OPTIMUM ABSORBER

For vibration suppression performance, we select the *m*ean-square *a*cceleration *r*esponse (MSAR) of the primary system. That is,

$$E\{(\ddot{\bar{x}}_1)^2\} = \int_0^\infty |H(\mathrm{i}\omega)|^2 S(\omega)\,\mathrm{d}\omega, \tag{6}$$

where $S(\omega)$ is the power spectral density of the excitation force $f(t)$, and H is defined in equation (5).

As depicted in Figure 1, this optimization is carried out in three options: semi-active adjustment (only over **p**), or active re-tuning (only over **u**), or hybrid treatment (over both **p** and **u**). For this process, we assume that the structural properties are fixed and known. In practice, however, the structural variations will affect the optimum absorber performance, and therefore, the approach to obtain optimum absorber performance may be mixed with the application of system identification techniques. This is explained later in section 4.

We briefly describe the optimization iterations used in these three options, with their specific cost function and constraints detailed in the following sections (Sections 3·1–3·3). In general, we seek an optimum parameters vector, **v**, such that the MSAR of the primary system is minimized over a desired range of **v** and subject to some physical and stability constraints.

The initial values of the parameters, $\mathbf{v}^{(0)}$, start the optimization process. The optimum value of the absorber parameter, $\mathbf{v}^*$, is numerically determined next, in such a way that the cost function.

$$J = \min_{\mathbf{v}} \{E[(\ddot{\bar{x}}_1)^2]\} = \min_{\mathbf{v}} \{G(\mathbf{v})\} \tag{7}$$

subject to m number of generic constraints

$$h_i(\mathbf{v}) \leqslant 0, \quad i = 1, 2, \ldots, m \tag{8}$$

is minimized.

For a procedural simplification, this *constrained* optimization problem can be converted to an *unconstrained* optimization using a transformation described in reference [13]. That is, we convert the constrained optimization problem (7, 8) into the unconstrained problem

$$G_{new}(\mathbf{v}, \mathbf{r}) = G(\mathbf{v}) + Q(\mathbf{h}(\mathbf{v}), \mathbf{r}), \tag{9}$$

where **r** is a vector of penalty imposing parameters and $\mathbf{h} = \{h_i(\mathbf{v}),\ i = 1, 2, \ldots\}$. Q is a real-valued function whose contribution to the objective function (G_{new}) is controlled by **r**. The form of this additional penalty can be appropriately selected. Here we use the "*Inverse Barrier Function*" of reference [13],

$$Q(\mathbf{h}(\mathbf{v}), r) = (1/r) \sum_{i=1}^{m} [-1/h_i(\mathbf{v})], \tag{10}$$

where r is taken as a positive scalar. It is clear that, as the parameter **v** gets closer to the constraint, h_i becomes smaller increasing the value of Q rapidly. The function Q becomes infinite if any one of the inequality boundaries becomes active. Thus, if the iterative process starts from a feasible point it does not go into the infeasible region because of the huge barrier. It is shown that as $r \to \infty$ (i.e., $Q \to 0$), $\mathbf{v}^*_{new} \to \mathbf{v}^*$ and the minimum of the objective function $G_{new}(\mathbf{v}, r)$ is reached. The $\mathbf{v}^*$ is the optimum solution of the original constrained optimization problem.

Since the computation of the higher derivatives of the objective function G_{new} may be very complicated in some applications, we deploy the optimization techniques which use inferior information: the *direct update methods*. These methods require the computation of only first derivatives of the cost function. Using the information obtained from the previous iterations, convergence towards the minimum is accelerated. In this study, we follow the

Broyden–Fletcher–Goldfarb–Shanno (**BFGS**) method which has been proved to be the most effective in similar applications. We refer the interested reader to Gill *et al.* [13] for detailed derivations of this method, and applied to delayed feedback vibration absorber in reference [14].

3.1. OPTIMIZATION IN SEMI-ACTIVE SUBSECTION (FIGURE 1, PORT 1)

The optimization problem in this unit is performed over the adjustable absorber properties (i.e., $\mathbf{v} = \mathbf{p}$). The utilization of the smart structures such as EM/MR dampers or magnetostrictive materials (Terfenol-D, for instance) provides an adjustable suspension system (here, variable damper c_a and stiffness k_a) [15, 16]. Hence, an attempt is made to

$$\min_{\mathbf{p}} \{E\{(\bar{\ddot{x}}_1)^2\}\} \tag{11}$$

over only the variable structural parameters $\mathbf{p} = \{c_a\ k_a\}^{\mathrm{T}}$, while $u = 0$, and subject to physical constraints

$$\mathbf{p}^{low} \leqslant \mathbf{p} \leqslant \mathbf{p}^{up}. \tag{12}$$

The lower and upper bounds are chosen considering some practical limitations. The resulting optimum design will be utilized in the active subsection for further improvement.

3.2. OPTIMIZATION IN ACTIVE SUBSECTION (FIGURE 1, PORT 2)

Using the optimum structural parameters found in the preceding section, a second optimization, over the control parameters $\mathbf{u}$ (i.e., $\mathbf{v} = \mathbf{u}$), is conducted to further minimize the MSAR. Notice, $\mathbf{p}$ is kept fixed in this step. That is, we seek the control parameters $\mathbf{u}$ to

$$\min_{u} \{E\{(\bar{\ddot{x}}_1)^2\}\} \tag{13}$$

and subject to

$$\mathbf{u}^{low} \leqslant \mathbf{u} \leqslant \mathbf{u}^{up}, \text{ assurance of system stability, and } \int_0^\infty u^2(t)\,\mathrm{d}t \leqslant D, \tag{14}$$

where D is a desired measure of the power requirement.

Notice that in the semi-active unit, the absorber is always stable. The stability assurance arises when active control is used. As the control parameters vector, $\mathbf{u}$, is used for optimization, their influence on the system stability should be studied in parallel.

It is expected that the concurrent optimization over structural properties and control parameters may lead to a better performance, due to the additional parameters and hence added flexibility in the optimization iterations [17].

3.3. CONCURRENT OPTIMIZATION IN SEMI-ACTIVE AND ACTIVE SUBSECTIONS (FIGURE 1, PORT 3)

As outlined earlier, the concurrent optimization provides more flexibility in selecting optimum parameters and satisfying the constraints. Hence, the numerical problem

encountered here is to find the variable absorber parameters **p** and control parameters **u**, which minimize the MSAR of the primary system. As such, we seek the optimal absorber parameters $\mathbf{v} = [\mathbf{p}\ \mathbf{u}]^{\mathrm{T}}$ to

$$\min_{\mathbf{v}} \{E\{(\bar{x}_1)^2\}\} \tag{15}$$

subject to the physical bounds, stability and power-consumption constraints (expressions (12) and (14)).

The stability constraint may change simultaneously in each optimization iteration, if it depends on the absorber parameters (which happen to be a part of the parameters vector sought). In the numerical section, we will demonstrate this with an example case study where this dependency is included in the iterations.

The above options are decided through the 2nd interpretation in the signal flow of the scheme (Figure 1). A designer can decide on the suitability of each approach and a set of feasible design algorithms can be created. This new flexibility, its influence on the vibration suppression and end effects will create a vehicle for further research and study.

4. RE-TUNING PROPOSITION

If structural parameters show variations, the active unit can be utilized to compensate for these variations. This operation does not constitute a total overhaul of the structure. Thus, it does not impose high costs and interruption of service, yet it brings the most desirable vibration suppression conditions possible to the system even though the structural features have substantial variations from their nominal design values [17].

A method that uses only absorber acceleration is proposed here. This signal should be sufficient to identify the parametric variations in the structure. Imagine that an excitation $f(t)$ and the control parameters **u** are applied to both the true plant (or experimental set-up) and the nominal plant, as shown in Figure 3. $H_P^*(\boldsymbol{\theta}^*)$ and $H_P(\boldsymbol{\theta})$ are the transfer operators of the true and the model plants respectively.

The objective of the parameter identification is to minimize the difference between true absorber acceleration output, $\ddot{x}_a^*(t)$, and nominal absorber acceleration output, $\ddot{x}_a(t)$, by

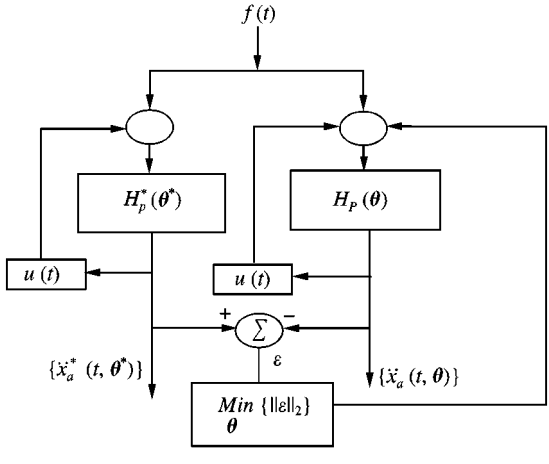

Figure 3. Schematic of the identification objective.

properly selecting the system parameters $\boldsymbol{\theta}$. The problem can be stated using a cost function

$$J_{ID} = \min_{\boldsymbol{\theta}} \{ \| \ddot{x}_a^*(t, \boldsymbol{\theta}^*) - \ddot{x}_a(t, \boldsymbol{\theta}) \| \} \tag{16}$$

subject to the physical constraint

$$\boldsymbol{\theta} > \mathbf{0} \tag{17}$$

and the inequality bound

$$\left\| \frac{\boldsymbol{\theta}}{\bar{\boldsymbol{\theta}}} - \mathbf{1} \right\| \leqslant \psi. \tag{18}$$

The nominal absorber acceleration is obtained by solving differential equations (1) and (2) with nominal parameters, $\boldsymbol{\theta} = \bar{\boldsymbol{\theta}}$. It is also assumed that $\bar{\boldsymbol{\theta}}$ satisfies inequality (3). The parameter $\boldsymbol{\theta}$ is then numerically updated in such a way that the cost function described in equation (16), subject to constraints (17) and (18), is minimized.

5. NUMERICAL RESULTS AND SIMULATIONS

The optimization processes described earlier for vibration absorption and parameter identification are combined. We assume that the nominal system parameters are available and satisfy inequality (18). It is also assumed that the absorber acceleration is available as measured data. The primary system is taken as a s.d.o.f. structure which is subjected to a wide-band frequency load in the interval of $\omega \in [400, 1500]$ Hz. The absorber is appended to it, and the resulting combined structure is shown in Figure 2(b). The primary system parameters are taken as $m_1 = 5{\cdot}77$ kg, $k_1 = 251{\cdot}132 \times 10^6$ N/m, $c_1 = 1142{\cdot}0$ kg/s. This system has a peak frequency at $\omega_{peak} = 1050$ Hz. The absorber mass to primary mass ratio is taken to be 3·9% ($m_a = 0{\cdot}227$ kg).

The control law is in the form of delayed acceleration feedback as fully discussed in reference [14] and summarized in Appendix A:

$$u(t) = g\ddot{x}_a(t - \tau), \tag{19}$$

where g and τ are the feedback gain and time delay respectively. The reason for taking this format is the simplicity of the control implementation since it requires partial state feedback only (here absorber acceleration). The control parameter $\mathbf{u}$ is, therefore, expressed in the form of $\mathbf{u} = \{g, \tau\}$.

The signal flow of Figure 1 is followed.

Using the given physical parameters, the optimal semi-active absorber (OSA) (i.e., $u = 0$) is found first: $\bar{k}_a = 9{\cdot}7915 \times 10^6$ N/m and $\bar{c}_a = 305{\cdot}6264$ kg/s, with $\min\{MSAR\} = 2332{\cdot}2$. This is the semi-active adjustment only as described in section 3.1. The resulting optimum semi-active absorber is considered to start further improving the performance characteristics in the active unit. Keeping $\bar{k}_a$ and $\bar{c}_a$ fixed, a 2-D optimization is performed over g and τ. This yields the control parameters of $\bar{g} = 0{\cdot}0084$ kg, $\bar{\tau} = 0{\cdot}7102 \times 10^{-3}$ s, with $\min\{MSAR\} = 2308{\cdot}5$. This setting is named optimum active based on an optimum semi-active absorber (OA–OSA). This is an active retuning only option as per section 3.2. The full-scale optimization problem over $[k_a, c_a, g, \tau]^{\mathrm{T}} \in \Re^4$ is handled next, yielding

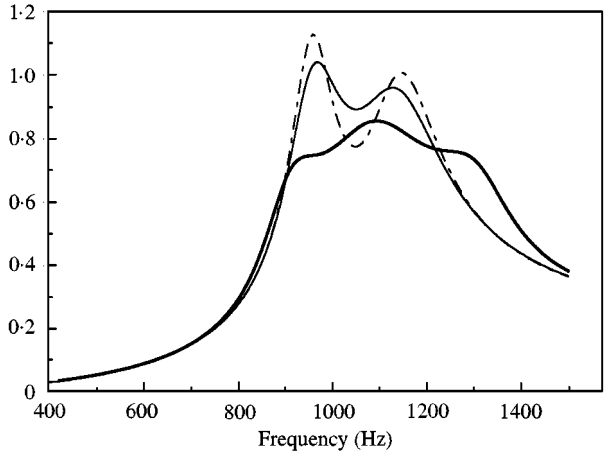

Figure 4. The non-dimensional true frequency responses (primary acceleration to excitation force) for different settings: (– · – · – · – · – · –), OSA with max peak response of 1·123; (——), OA–OSA with max peak response of 1·037; (——), OHA with max frequency response of 0·860.

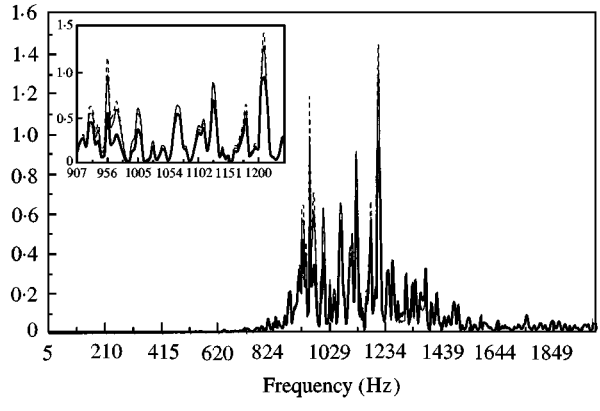

Figure 5. The non-dimensional power spectral density of the primary system acceleration for different settings: (– · – · – · – · – · –), OSA with max peak response of 1·434; (——), OA–OSA with max peak response of 1·291; (——), OHA with max frequency response of 0·956.

$\mathbf{v}^* = [k_a = 9{\cdot}6639 \times 10^6,\ c_a = 14{\cdot}23,\ g = 0{\cdot}0492,\ \tau = 0{\cdot}7226 \times 10^{-3}]^{\mathrm{T}}$ and $\min\{MSAR\} =$ 2079·0. This is called the optimum hybrid absorber (OHA), as discussed in section 3.3.

In order to display the improvement in the vibration absorption, the frequency response of the primary system with OSA, with OA–OSA, and with OHA are shown in Figure 4. The OHA delivers better than 23% improvement in the vibration suppression over the OSA (for this example), while the optimum active absorber based on optimum semi-active parameters offers only about 8% improvement (notice the insignificant difference in MSAR of OSA and OA–OSA settings). This is the best stable absorber setting based on the calculated semi-active absorber, and it seems the addition of the active feature does not improve the system response as much as hybrid treatment does.

This demonstrates that concurrent adjustment of structural properties (absorber stiffness and damping) and control parameters (g and τ) offers a significant improvement over separate treatment in each subsection. This highlights the importance of the interpretation

mentioned. The corresponding stability is also assured and both optimum solutions (OA–OSA and OHA) fall in the feasible regions.

In order to demonstrate the performance characteristics, i.e., the MSAR of the primary system (cost function criterion in optimization loop), the power spectral density of the primary acceleration is shown in Figure 5. The number of recorded data is 2048, with the sampling time of 0·0001 s. Notice the close correspondence of Figures 4 and 5 from the frequency spectrum viewpoint. The discrepancy between these two plots is originated from the problems associated with wide-band signals in the frequency domain [18, 19].

For the time domain representation, the excitation force is considered to have a white-band spectral density. The ratio of the corresponding power spectral density is not equal to the true frequency transfer function, as it is obvious from Figures 4 and 5. This is the reason why the identification in this study is done in the time domain. The aim of giving these spectra, here, is just to show the trend of improvement of the vibration suppression in different settings.

5.1. FEASIBILITY OF THE RE-TUNING PROPOSITION

Imagine that structural properties deviate from their nominal design values over time. This de-tuning is a common occurrence in industry, which brings sub par vibration suppression performance. The proposed technique handles the re-tuning procedure in active or semi-active unit through the interpretation mentioned. This will bring the best performance characteristic despite these parametric variations [17].

The two optimization processes described earlier (one for identification and the other for vibration absorption) are now combined together. For simplicity, it is aimed that this retuning procedure be performed through the active unit only (over $\mathbf{u}$). This avoids changes in the semi-active unit (damper and stiffness), which may be undesirable in some applications. In order to identify the system parameters $\boldsymbol{\theta}$, corresponding to the true absorber acceleration, we freeze a segment of the data and implement the system identification optimization. This step is followed by the optimization on g and τ based on the newly identified parameters. The number of iterations for each optimization is controlled such that the execution time is kept below a certain value. This duration can be appropriately selected by the user. As soon as the new control parameters become available they are implemented on the true plant and a new segment of data is collected to repeat this procedure. Since the convergence towards the true system parameters, $\boldsymbol{\theta}^*$, is guaranteed [17], this repetition improves the quality of the identification.

For the simulation purpose, we consider step type variations on the parameters k_a, c_a, k_1, and c_1 from their nominal (estimated) values, $\bar{k}_a$, $\bar{c}_a$, $\bar{k}_1$, and $\bar{c}_1$. It is clear that variations in these parameters are likely to happen much more frequently than those of m_a and m_1. Therefore, the masses are taken as time-invariant quantities. For a numerical example we assume that the nominal values are arbitrarily perturbed as

$$k_a^* = 1{\cdot}10\,\bar{k}_a, \quad c_a^* = 1{\cdot}10\,\bar{c}_a, \quad k_1^* = 1{\cdot}05\,\bar{k}_1, \quad c_1^* = 1{\cdot}05\,\bar{c}_1, \quad m_a^* = \bar{m}_a, \quad m_1^* = \bar{m}_1. \tag{20}$$

When the resultant OHA setting (based on the nominal values, $\bar{\boldsymbol{\theta}}$) is used for this perturbed system, the discrete Fourier spectrum (DFS) of the primary system deteriorates considerably (thin lines in Figure 6). This is the *de-tuned* situation, with the values given by

$$g^{(de\text{-}tuned)} = 0{\cdot}0492\ \text{kg}, \ \tau^{(de\text{-}tuned)} = 0{\cdot}7226\ \text{ms for true system parameters } \boldsymbol{\theta}^*. \tag{21}$$

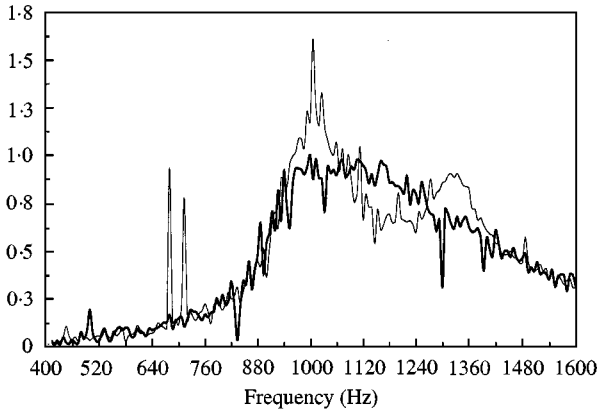

Figure 6. The non-dimensional discrete Fourier spectra of the primary system acceleration for de-tuned (——) and re-tuned (———) settings.

It is clear that one of the resonant peaks dominates while the other is not apparent. That is, the absorber is no longer an optimum one for the present primary. When the system identification and absorber optimization steps are taken as per section 4, the *re-tuned* (i.e., optimum) setting is reached as

$$g^{(re\text{-}tuned)} = 0{\cdot}0533 \text{ kg}, \tau^{(re\text{-}tuned)} = 0{\cdot}6721 \text{ ms for true system parameters } \boldsymbol{\theta}^*, \qquad (22)$$

which yields a much better frequency response (see thick lines in Figure 6).

The peak frequency responses for the primary system with de-tuned and re-tuned settings are shown in Figure 6. It is obvious that the re-tuned absorber delivers considerable improvement (better than 22% for this set of data) in the vibration suppression over the de-tuned absorber.

This demonstrates the capability of the suggested semi-automated methodology for the example given in this work. The challenge lies in implementing this scheme for complex primary systems. If successful, however, this strategy can offer a substantial boost to industries which use vibration absorbers heavily.

6. CONCLUDING REMARKS AND FUTURE DIRECTIONS

Commonly used passive vibration absorbers become de-tuned over time due to the structural variations. In order to compensate for these deviations, active vibration suppression schemes are needed. These techniques, however, suffer from the control-induced instability in addition to the large-control effort requirement. A semi-automated approach is presented to improve the wide-band frequency response of a structure. The proposed strategy utilizes semi-active and active subsections, in which structural properties and control parameters are adjustable. By altering these features a vehicle for further study on the adjustment configuration and intelligent interpretations is created. Through simulations, it is shown that the concurrent adjustment of structural properties and control re-tuning significantly improves the vibration suppression quality. An essential component of this strategy is handling the parametric variations within the system. In order to increase the absorber efficiency against such variations an identification

process is utilized in sequence with an optimization for re-tuning the absorber. These features are very important and will broaden the utility of the vibration absorbers in industrial applications where a wide range of structural variations is encountered.

The most critical component of the proposed study, i.e., supervisory decision-making for semi-automated operation, is currently being studied. The main contribution of this study is introducing this interpretation process and demonstrating its feasibility and possible configurations through simulations. The predominant activity will be around developing and facilitating this interpretive decision-making process via numerical tools, and when implemented on realistic systems with complex dynamics and controllability.

REFERENCES

1. J. Q. Sun, M. R. Jolly and M. A. Norris 1995 *ASME Special* 50*th Anniversary*, *Design issue* **117**, 234–242. Passive, adaptive, and active tuned vibration absorbers—a survey.
2. M. Abe and T. Igusa 1996 *Journal of Sound and Vibration* **198**, 547–569. Semi-active dynamic vibration absorbers for controlling transient response.
3. D. Margolis 1998 *Journal of Vibration and Acoustics* **120**, 104–110. Retrofitting active control into passive vibration isolation systems.
4. E. Esmailzadeh and N. Jalili 1998 *ASME Journal of Vibration and Acoustics* **120**, 833–841. Optimal design of vibration absorbers for structurally damped Timoshenko beams.
5. N. Olgac and N. Jalili 1999 *Smart Structures* **65**, 237–246. Optimal delayed feedback vibration absorber for flexible beams.
6. C. L. Giliomee and P. S. Els 1998 *Journal of Terramechanics* **35**, 109–117. Semi-active hydropneumatic spring and damper system.
7. M. Nagarajaiah 1997 *Proceedings of Structural Congress*, *ASCE*, *Portland*, OR, 1574–1578. Semi-active control of structures.
8. D. Nemir, Y. Lin and N. Osequeda 1994 *ASCE Journal of Structural Engineering* **120**, 423–429. Semi-active motion control using variable stiffness.
9. G. J. Lee-Glauser, G. Ahmadi and L. G. Horta 1997 *ASCE Journal of Structural Engineering* **123**, 499–504. Integrated passive/active vibration absorber for multistory buildings.
10. T. T. Soong and M. C. Constantinou 1994 *Passive and Active Structural Control in Civil Engineering*. Wien and New York: Springer-Verlag.
11. W. Kortum, W. Schiehlen and M. Hoffmann 1994 *Vehicle System Dynamics* **23**, 274–296. Progress in integrated system analysis and design for controlled vehicles.
12. A. G. Thompson 1976 *Vehicle System Dynamics* **5**, 187–203. An active suspension with optimal linear state feedback.
13. P. E. Gill, W. Murray and M. H. Wright 1981 *Practical Optimization*. New York: Academic Press.
14. N. Jalili and N. Olgac 2000 *ASME Journal of Dynamic Systems*, *Measurements*, *and Control* **121**, 314–321. A sensitivity study of optimum delayed feedback vibration absorber.
15. J. Shaw 1998 *Journal of Intelligent Material Systems and Structures* **9**, 87–94. Adaptive vibration control by using magnetostrictive actuators.
16. E. Garcia, J. Dosch and D. J. Inman 1992 *Journal of Intelligent Material Systems and Structures* **3**, 659–667. The application of smart structures to the vibration suppression problem.
17. N. Jalili and N. Olgac 2000 *AIAA Journal of Guidance*, *Control*, *and Dynamics* **23**, 1–10. Identification and re-tuning of optimum delayed feedback vibration absorber.
18. R. Pintelon, J. Schoukens and G. Vandersteen 1997 *IEEE Transactions on Automatics Control* **42**, 1717–1720. Frequency domain system identification using arbitrary signals.
19. P. Pintelon, P. Guillaume, Y. Rolain, J. Schoukensand and H. Van Hamme 1994 *IEEE Transactions on Automatic Control* **39**, 2245–2260. Parametric identification of transfer functions in the frequency domain—a survey.
20. N. Olgac and B. Holm-Hansen 1994 *Journal of Sound and Vibration* **176**, 93–104. A Novel active vibration absorption technique: delayed resonator.
21. N. Olgac, H. Elmali, M. Hosek and M. Renzulli 1997 *ASME Journal of Dynamic Systems*, *Measurements*, *and Control* **119**, 380–388. Active vibration control of disturbed systems using delayed resonator with acceleration feedback.

APPENDIX A: DELAYED FEEDBACK VIBRATION ABSORBER, AN OVERVIEW

An extension to the earlier work on the delayed resonator [20] is the delayed feedback vibration absorber (DFVA) [14]. As per Figure 2(b), a conventional passive absorber is reconfigured using a delayed acceleration feedback. The corresponding new system dynamics is the same as per equations (1) and (2) with the control law given by equation (19). By properly selecting the control parameters g and τ, the dominant roots can be moved anywhere off the imaginary axis. This general DFVA lends itself to an optimization process for the most desirable location of these dominant roots.

The transfer function between the excitation force and primary system acceleration is then written as

$$TF(s) = \frac{s^2 X_1(s)}{F(s)} = s^2 \left\{ \frac{m_a s^2 + c_a s + k_a - g s^2 \mathrm{e}^{-\tau s}}{H(s)} \right\}, \tag{A.1}$$

where

$$H(s) = \{m_1 s^2 + (c_1 + c_a)s + k_1 + k_a\}(m_a s^2 + c_a s + k_a - g s^2 \mathrm{e}^{-\tau s})$$
$$- (c_a s + k_a)(c_a s + k_a - g s^2 \mathrm{e}^{-\tau s}).$$

Notice, the characteristic equation of the combined system is simply

$$H(s) = 0. \tag{A.2}$$

For each $g \neq 0$ and $\tau \neq 0$, equation (A.2) has an infinite number of roots. The passive absorber, i.e., $g = 0$, is always stable while a DFVA with improper selection of gain and delay can drive the system to instability.

The necessary and sufficient condition for asymptotic stability is that the roots of the characteristic equation (A.2) all have negative real parts. This equation is transcendental and presents infinitely many finite roots. Therefore, the verification of the root locations is not a trivial task. In order to resolve this, a *stability chart strategy* is used as described in reference [21]. It is easy to recast the characteristic equation (A.2) into the form

$$g\mathrm{e}^{-\tau s} = \frac{N(\boldsymbol{\theta}, s)}{D(\boldsymbol{\theta}, s)}, \tag{A.3}$$

where N and D are polynomials of s.

When the combined system is marginally stable, there are at least two roots of the characteristic equation on the imaginary axis, i.e., $s = \pm \mathrm{j}\omega_{cs}$, $j = \sqrt{-1}$ (subscript "cs" denotes the combined system). Introducing this condition into equation (A.3) yields the necessary control parameters

$$g_{cs} = \left| \frac{N(\boldsymbol{\theta}, \omega_{cs}\mathrm{j})}{D(\boldsymbol{\theta}, \omega_{cs}\mathrm{j})} \right|, \tag{A.4}$$

$$\tau_{cs} = \frac{1}{\omega_{cs}} \left\{ (2\ell - 1)\pi + \angle \frac{N(\boldsymbol{\theta}, \omega_{cs}\mathrm{j})}{D(\boldsymbol{\theta}, \omega_{cs}\mathrm{j})} \right\}, \quad \ell = 1, 2, \ldots, \tag{A.5}$$

where $\|$ and $\angle$ are the magnitude and the angle of the arguments respectively.

For a particular delay $\tau = \tau_0$, the combined system crossings, $\omega_{cs\ell}(\tau_0)$, are determined from equation (A.5) and the corresponding gains, $g_{cs\ell}$, from equation (A.4), where the subscript and counter $\ell = 1, 2, \ldots$ refers to the first, second, etc., root loci branch crossings. To ensure stability of the system, the feedback gain g should be smaller than the infimum of these $g_{cs\ell}(\omega_{cs\ell})$ values [20, 21]. That is,

$$g < g_{min}(\omega_{cs\ell}(\tau_0)), \tag{A.6}$$

where

$$g_{min} = infemum \begin{Bmatrix} g_{cs}(\omega_{cs1}) \\ g_{cs}(\omega_{cs2}) \\ g_{cs}(\omega_{cs3}) \\ \vdots \end{Bmatrix} \quad \text{for } \tau = \tau_0. \tag{A.7}$$

These operating points, $\{\min g_{cs\ell}, \tau_{cs\ell}\}$, $\ell = 1, 2, \ldots$, form the marginal stability boundary for the combined system, below which (i.e., $g_{cs} < \min g_{cs\ell}$) the system is stable, and above unstable [20, 21]. This stability boundary between the infeasible and feasible regions is numerically determined using equation (A.7) and used in the optimization iterations, for the assurance of the stability (expression (14)).